

The production of drops by the bursting of a bubble
at an air liquid interface

J.S. Darrozès and P. Ligneul
Université Paris VI, Campus Univ. Bat 502 Orsay, Orsay, FRANCE 91405

Abstract

This work describes the fundamental mechanism arising during the bursting of a bubble at an air-liquid interface. A single bubble is followed from an arbitrary depth in the liquid, up to the creation and motion of the film and jet drops. Several phenomena are involved and their relative order of magnitude is compared in order to point out the dimensionless parameters which govern each step of the motion. Furthermore, this study is completed by high speed cinematography. The characteristic bubble radius which separates the creation of jet drops from cap bursting without jet drops is shown to be $a = (\sigma/\rho g)^{1/2}$. The corresponding numerical value for water is 3 mm and agrees with experimental observations.

Introduction : physical mechanisms description

The burst of gas bubbles on a liquid interface leads to a mass transfer in stratified two-phase flows which is of great importance in many fields such as ocean-atmosphere exchanges, aerosol generation, boilers, degazeification processes, etc... The physical mechanisms of such a phenomenon are still not wellknown. The burst occurs during a few tens of microseconds and involves many physico-chemical effects. The film cap draining is due to gravity and surface tension and its thickness (in the range of 0.5 to 10^{-3} micrometers) may be small enough to produce non negligible intermolecular forces which depend on the impurities contained in the liquid phase. The film cap breakage generates an aerosol which is usually split into two distinct families which are the "film drops" and the "jet drops".

. The film drops are created by the tearing of the interfacial cap which propagates from an initial hole at a very high speed (8 m/s). Due to the tangential motion of the liquid film, some drops are ejected horizontally and the others are blown vertically by the air which was initially inside the bubble. Another possible mechanism is the sudden shattering of the whole cap which bursts into droplets in any direction. Film drops are very small (1 - 20 μm) and their number increases with the initial bubble diameter ϕ_b (about 100 when $\phi_b = 2$ mm, and 1000 when $\phi_b = 6$ mm). They are ejected up to a height in the order of 10 to 20 mm above the free surface level.

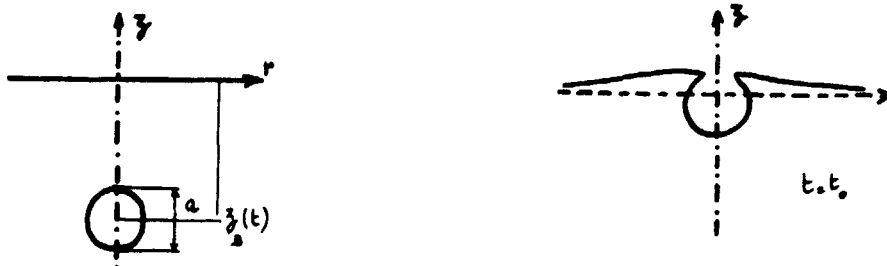
. The jet drops are produced by the very fast motion of the bubble bottom interface which is in a state of non-equilibrium when the film cap breaks. Instantaneously, gravity and surface tension act to create a strong interface deformation and give rise to the formation of a jet in the upward direction. Because of instabilities, the liquid jet is fragmented into several drops (from 1 to 5 depending on the bubble diameter ϕ_b , in the range 6 mm to 0.1 mm). For values of ϕ_b less than 2 mm, the ejection height of jet drops may reach 100 ϕ_b above the free surface level.

These two families lead to a transfer in the gas of two different kinds of chemical substances, namely the surfactants spread on the free surface (film drops) and the particules in suspension or dissolved inside the liquid (jet drops).

The aim of this paper is to consider a dimensional analysis of aerosol production in order to reach a better understanding of the phenomena involved during the bursting of the bubble. The notion of dimensionless parameters, characteristic times and predominant mechanisms may be used to define simplified experimental studies and to search for approximate analytical solutions. In what follows, several effects are analyzed :

- underwater bubble rising - film drainage - cap tear propagation
- film drops ejection - free surface motion after film cap rupture.

Underwater bubble rising



The dimensionless form of equations governing the relative liquid flow past the bubble is written with the characteristic bubble size a , the pressure variation $\rho a g$ (involving the liquid density ρ and the acceleration g gravity) and an unknown characteristic time τ which leads to the reference velocity a/τ . The bubble motion is obtained from the fundamental dynamic law :

$$F = \iint_{ab} \left[-p_{loc} \frac{1}{a} + \frac{2v}{g\tau a} \underline{D} \cdot \underline{n} \right] \cdot \underline{n} ds = 0 \quad (1)$$

in which the symmetric part \underline{D} of the velocity gradient $\underline{\nabla v}$ and the local pressure p_{loc} are given by the Navier-Stokes equation :

$$\frac{d^2 z_B}{dt^2} + \frac{dv}{dt} + \nabla(p_{loc} - z) \frac{g\tau^2}{a} = \frac{v\tau}{a^2} \Delta v \quad (2)$$

The bubble shape is deduced from the normal stress equilibrium

$$p_i = p_{loc} + \frac{p_a}{\rho g a} + z_B(t) - \frac{2v}{g\tau a} (\underline{D} \cdot \underline{n}) \cdot \underline{n} + \frac{4\sigma}{\rho g a^2} C \quad (3)$$

\underline{n} is the unit normal vector, p_i , C , v and σ respectively stand for the internal bubble pressure, the mean curvature, the dynamic viscosity and the surface tension coefficient.

The local pressure is defined by the relation

$$p = \frac{p_a}{\rho g a} + z_B(t) + p_{loc}$$

in which, for the most part, the constant $p_a/\rho g a$ is much greater than unity.

It is easily seen, from equation (2), that high Reynolds number flows correspond to the characteristic time evolution $\tau_g = (a/g)^{1/2}$, and situations dominated by viscous effects are scaled by the reference time $\tau_v = \nu/ag$. The relative Reynolds number :

$$R_r = a^3 g / \nu^2 = (a/a_1)^3 \quad (4)$$

leads to a characteristic length $a_1 = (\nu^2/g)^{1/3}$ ($\sim 50 \mu\text{m}$ for water). In equation (3), another length $a_2 = 2(\sigma/\rho g)^{1/2}$ ($\sim 6 \text{ mm}$ for water) is defined from the dimensionless number :

$$\Sigma = 4\sigma/\rho g a^2 = (a_2/a)^2 = (\tau_g/\tau_s)^2 \quad (5)$$

The new characteristic time $\tau_s = \rho a^3/4\sigma$ concerns the interface vibrations due to the surface tension. Depending on the bubble diameter a , the following situations occur.

. $a \gg a_2$, $R_r \gg 1$, motions due to surface tension are frozen, but the bubble can oscillate with instationary terms of equation (3) (bubble wake for instance) on the time scale τ_g .

. $a_1 \ll a \ll a_2$, $R_r \gg 1$ but the non stationary terms in equation (3) are negligible and the bubble keeps its spherical shape.

. $a \ll a_1$, $R_r \ll 1$ and the comparison between the last two terms of equation (3) leads to a new length $a_3 = \rho \nu^2/2\sigma$ ($\sim 5 \cdot 10^{-3} \mu\text{m}$ for water). Bubble diameters less than a_3 will not be considered in this paper. Therefor surface tension is the dominant phenomenon and deformations cannot occur. We will write $\pi = a_3/a = \rho \nu^2/2\sigma a$ (always less than unity for water).

The characteristic velocities of the rising motion are $(ag)^{1/2}$ when $a > a_1$ and $\frac{1}{18} \frac{a^2 g}{\nu}$ (stokes drag) when $a < a_1$.

Film draining

There are two fundamental mechanisms which cause the film draining, when the bubble arrives on the free surface. First, the gravity which creates the bubble motion and inertia terms (when $a > a_1$) increases the local pressure p_a on the free surface. On the relative stagnation point, this increase is of the order of $\rho g a$. Secondly, the free surface curvature leads to a pressure increment in the order of $4\sigma/a$. Comparison between both phenomena

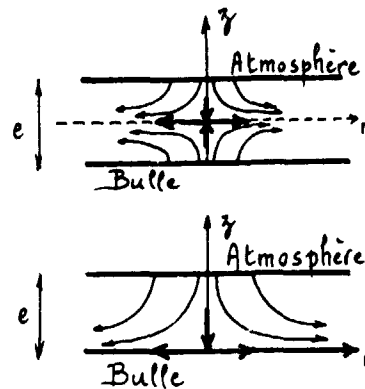
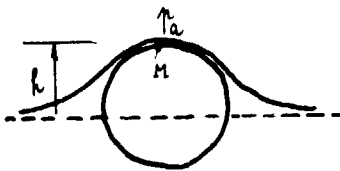
is given by the value of $\Sigma = 4\sigma/\rho a^2$ introduced in the last paragraph. Consequently, for bubble diameters larger than a_2 , the effect of gravity is predominant, and for $a_1 \ll a \ll a_2$ the surface tension plays the most important role.

A very crude analysis for $\Sigma \ll 1$ shows that (from the continuity equations) the liquid pushed up by the rising of the bubble (order $\frac{\pi}{4} a^2 \sqrt{ag}$) must be evacuated through the lateral surface of a cylinder ($\pi a h \sqrt{ag}$). This balance gives an order of magnitude of the height below the free surface which must be reached by the bubble top before undergoing a non negligible free surface deformation. When $a_1 \ll a \ll a_2$, the characteristic bubble rising velocity \sqrt{ag} has not the same order of magnitude as the characteristic velocity due to the surface tension pressure drop : $(4\sigma/\rho a)^{1/2}$ and the same crude analysis leads to :

$$\frac{\pi}{4} a^2 \sqrt{ag} = 2 \pi a h (\sigma/\rho a)^{1/2} \text{ and } h = \frac{a}{4\Sigma^{1/2}} \ll a$$

For very small bubble ($a_3 \ll a \ll a_1$), the same trivial argument gives :

$$h = a \pi^{1/2} \ll a$$



The characteristic draining time is easily deduced from the above considerations, and from the volume to be drained ($\sim \frac{\pi a^3}{16}$ when $\Sigma \ll 1$; $\frac{\pi a^3}{4\Sigma^{3/2}}$ when $a_1 \ll a \ll a_2$; and

$2 \pi a^3 \pi^{3/2}$ when $a \ll a_1$). One obtains respectively for each situation $\tau_d = \tau_g/4$, $\tau_g/2\Sigma$, $\sqrt{2} \tau_V \pi^{1/4} R_T$. As an example in each case, one obtains respectively for $a = 1$ cm, 1 mm and 10 μ m, the following values : $\tau_d = 0.07$ s, 4 ms and 0.5 ms, in water. The end of drainage in the first two cases is governed by viscous effects when the Reynolds number based on the

the film thickness e is of order unity i.e. $e \sim \nu/(ag)^{1/2}$ when $\Sigma \ll 1$ and $e \sim \nu(\rho a/\sigma)^{1/2}$ when $\Sigma \gg 1$. These limiting thicknesses in water are respectively 3 μ m and 0.3 μ m when $a = 1$ cm and $a = 1$ mm. At this stage, it is necessary to be very careful about the boundary conditions to be written on the film boundaries. For very dirty liquids, Haberman and Morton have shown that a vanishing velocity condition must be considered. In any case, one must take into account the influence of Van der Waals intermolecular forces which are, for a clean liquid, given under the form of a non isotropic tension in the normal direction to the film. Its value for a thickness e is (Sheludko):

$$\tau = \frac{4 \cdot 10^{-21}}{e^3} \text{ (MKSA units)}$$

this influence is non-negligible when the pressure gradient is of the same order :

$$a > a_2 (\Sigma \ll 1), \rho g \sim \frac{4 \cdot 10^{-21}}{e^4} \text{ and } e \sim \frac{5 \cdot 10^{-6}}{(\rho g)^{1/4}} = 0.5 \mu\text{m}$$

$$a < a_2 (\Sigma \gg 1), \frac{\sqrt{2}\sigma}{a^2 \Sigma^{1/4}} \sim \frac{4 \cdot 10^{-21}}{e^4} \text{ and } e \sim 10^{-5} a^{1/2} \text{ M.K.S.A. (0.3 } \mu\text{m when } a = 1 \text{ mm).}$$

These orders of magnitude for the film thickness is in agreement with the experimental evaluations.

Cap tear propagation



Assuming that a hole is created instantaneously, the driving force is due to surface tension and leads to a characteristic velocity : $v_f = (\sigma/\rho e)^{1/2}$. If the characteristic thickness $e \sim 1 \mu\text{m}$ is admitted, it follows that in water ($\sigma \sim 0.07$) the tear propagates with a velocity of 8 m/s which is exactly the value observed experimentally with a high speed camera. This evaluation is valid, only when the liquid flow inside the film is dominated by the inertia terms. This happens for a local Reynolds number greater than unity :

$$R_f = \frac{v_f e}{\nu} \gg 1 \rightarrow e \gg \frac{\rho \nu^2}{\sigma} \quad (= 0.01 \mu\text{m})$$

So, it is obvious that the experimental study of cap tear breaking may be performed without any precaution because any other phenomenon is frozen with respect to cap tear propagation. This has been done in the movie presented at the end of this paper.

This experiment shows the cap tear of a large bubble ($\phi_b = 4 \text{ cm}$) at rest on the free surface of ordinary drinkable water. The hole is created on the circle which delimits the bubble cap on the free surface. It is due to a much smaller bubble sticking to the larger one and which causes a point of weakness. Some papers (Vrij, Ivanov, ...) explain the film breaking by the non stable modes of capillarity waves, but this is probably true for bi-distilled water only.

Film drops ejection

The very complex nature of film cap fragmentation is not investigated in this paper, but we will consider the behaviour of a film droplet assumed to have a size in the order of $1 \mu\text{m}$

The blowing-out is due to the fact that the pressure level inside the bubble before breaking is larger than on the outside. The sudden pressure drop is of order $\rho_l a g$ when $\Sigma \ll 1$ and a/a when $\Sigma \gg 1$. For high Reynolds number gas flows, this produces velocities of order $(\rho_L a g / \rho_G)^{1/2}$ or $(\sigma/a \rho_G)^{1/2}$. For each case, the gas Reynolds number is :

$$R_G = \left(\frac{\rho_L g a}{\rho_G} \right)^{1/2} \frac{a^{3/2}}{\nu_G} \gg 1 \text{ if } a \gg 5 \mu\text{m} \quad (\text{air and water})$$

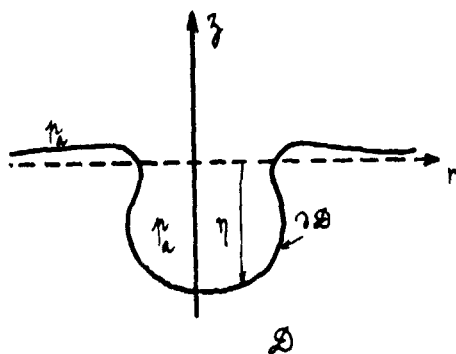
$$R_G = \left(\frac{\sigma a}{\rho_G \nu^2} \right)^{1/2} \gg 1 \text{ if } a \gg 0.1 \text{ \AA} \quad (\text{air and water})$$

The characteristic time of a particule transport due to the viscous drag is $\tau = \rho r^2 / \nu_G \rho_G$, where r denotes the particule radius. For a micronic droplet this time is 1 millisecond, as a result, film drops follow instantaneously the air flow produced by the breaking. For bubble diameters : 1 cm, 1 mm, 10 μm , the initial velocity of droplets are respectively : 10 m/s, 10 m/s and 100 m/s.

Experimentally, it is known that a 10 μm bubble does not produce any film drops, but one can see that for most bubbles, there is a strong interaction between the cap tear propagation (8 m/s) and the air ejection (10 m/s). If the air flow is roughly supposed to be similar to a source flow, the velocity V_r at a distance r is given by $V_r = V_1 (a/2r)^2$. A numerical value of V_r with $a = 1 \text{ mm}$ and $r = 1 \text{ cm}$ is 2.5 cm/s (less than 1 km/h). This argument proves that film drops are immediately convected by the wind in ocean-atmosphere exchanges.

Free surface motion after film cap rupture

It has been shown that film tear propagation occurs instantaneously with respect to the bubble rising velocity. This result confirmed by Mac Intyre's visualisations and by the photographs given in the present paper. As a result, the curvature of the bubble is greater at the bottom than the sides. This causes stronger surface tension forces on the deepest part of the bubble interface and produces the jet when the surface tension phenomenon is not negligible with respect to the gravity effect.



The dimensionless equations governing the free surface motion are written assuming a potential flow ($v = \nabla\phi$) for the liquid phase. It will be proved, later on, that inertia dominates the viscous terms. In a cylindrical coordinates system, the bubble diameter a is chosen as the reference length in the radial and vertical directions. The characteristic time T needed for the free surface $z = \eta(r, t)$ to reach an altitude of order a is unknown at this stage.

$$\frac{\phi_0}{T} \frac{\partial \phi}{\partial t} + \frac{\phi_0^2}{2a^2} (\nabla\phi)^2 + \frac{\sigma}{\rho a} \left(\frac{z}{a} - C \right) = 0 \quad (5)$$

$$\frac{a}{T} \frac{\partial \eta}{\partial t} + \frac{\phi_0}{a} \left(\frac{\partial \eta}{\partial r} \cdot \frac{\partial \phi}{\partial r} - \frac{\partial \phi}{\partial z} \right) = 0 \quad (6)$$

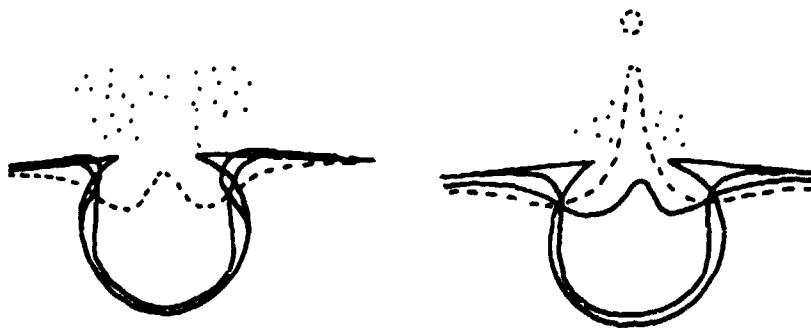
The reference potential ϕ_0 and the time T are obtained from the free surface boundary conditions. Equation (6) leads in any case to the relation $\phi_0 = a^2/T$. From equation (5), the characteristic time T depends on the comparison between $\Sigma^{-1} = \rho g a^2/4$ (gravity) and the mean dimensionless curvature C which is of order unity. $\Sigma \gg 1$: surface tension is the dominant phenomenon and $T = a\phi_0/\sigma = \rho a^3/\sigma T$. The characteristic time and velocity are respectively:

$$T = (\rho a^3/\sigma)^{1/2} \text{ and } V = (\sigma/\rho a)^{1/2}$$

$\Sigma \ll 1$: the free surface motion is governed by the gravity effect. One obtains respectively

$$T = (a/g)^{1/2} \text{ and } V = (ag)^{1/2}$$

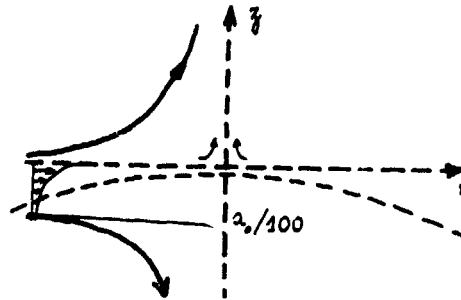
These results are valid only for high Reynolds number flows. When $\Sigma \gg 1$ ($a \ll a_2$, 0.6 cm for water) $R = aV/\nu = (a\sigma/\nu^2)^{1/2}$ which is larger than unity for bubble diameters larger than $a = \nu^2/\sigma$ (0.01 m for water). When $\Sigma \ll 1$, $R = (a^3g/\nu^2)^{1/2}$ and the bubble diameter must be larger than $a_1 = (\nu^2/g)^{1/3}$ (50 μm for water). This condition is always fulfilled because $a \gg 0.6$ cm.



The characteristic bubble diameter $a_2 = (4\nu/\sigma)^{1/2}$ splits the possible free surface behaviours into two classes:

$a > a_2$: the film cap rupture leads only to free oscillations of the free surface without jet, but many film droplets are blown into the atmosphere.

$a < a_2$: the predominance of the surface tension effect leads to a strong driving force at the bottom of the bubble which produces a jet. Surface tension forces still act on the jet surface and cause pressure gradients along the jet axis, oriented from the smallest sections to the largest ones. The draining of the lowest sections due to this mechanism leads to the jet breaking into one or several drops.



The dimensionless equation (5) shows that the gravity effect becomes important for a dimensionless z of order Σ . So the jet top can reach an altitude of order $a\Sigma$. The experimental evaluation : $100 a$, given in the introduction corresponds to $a = 0.6$ mm and an altitude of 60 cm. Dissipations due to viscous effects are given by the Reynolds number $R = (a_0/\rho v^2)^{1/2} \sim 8.10$ for a 0.6 mm bubble diameter. In that case, the boundary layer on the free surface, in which viscous draining occurs has a thickness in the order of a hundredth of a bubble diameter.

Flow visualisation

The photographs given in this section have been obtained with a high speed camera HYCAM (7500 images per second in the present case). The first sequence represents a cap tear which propagates on a 4 cm bubble diameter, from a small bubble (~ 1 mm) which was initially attached to the large one on the free surface. One can observe that some droplets tangentially ejected by the tear motion have a much larger size than 1 micrometer.

The next two sequences show jet drops due to a 1 mm bubble diameter. In "JET N°1", the hole created instantaneously by the breaking of the film is shown. The jet thickness is of order 0.1 mm corresponding to velocities of order $\sqrt{\sigma/\rho d_j} \sim 1$ m/s. The half-sphere in the upper part of each view is a liquid drop sticking on the end of a 1 mm cylindrical wire placed there to give an indication of the length scale. The "JET N°2" gives more details on the jet breaking mechanism. One can observe that the top drop has no motion during its growth, but its upward motion continues after its creation.

Concluding remarks

This paper is a first step in the study of aerosols created by bursting bubbles on an air-liquid interface. Jet drops have been studied and visualized in the past ; however a theoretical model for the prediction of the size and number of the drops would be useful for a better understanding of the jet breaking mechanisms.

Nevertheless, the lack of knowledge is more important for film droplets and a lot of experimental work will be necessary in order to visualize the film breaking and to predict the full size distribution of aerosols in a real industrial stratified two-phase flow figuration.

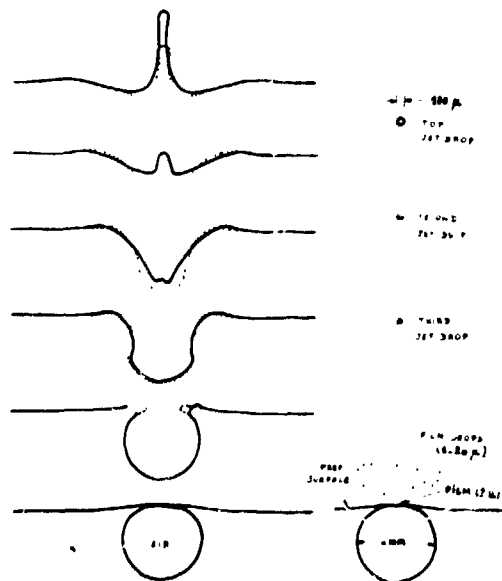
This study has been supported by a CNRS* contract.

* Centre National de la Recherche Scientifique (France).

ORIGINAL PAGE IS
OF POOR QUALITY

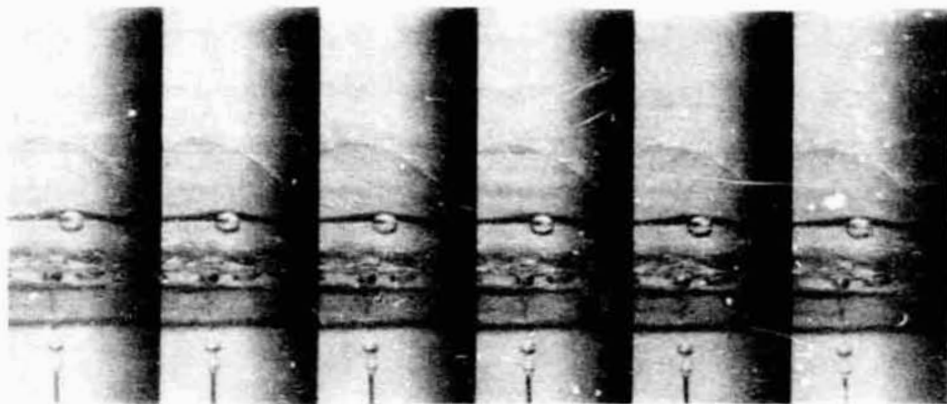
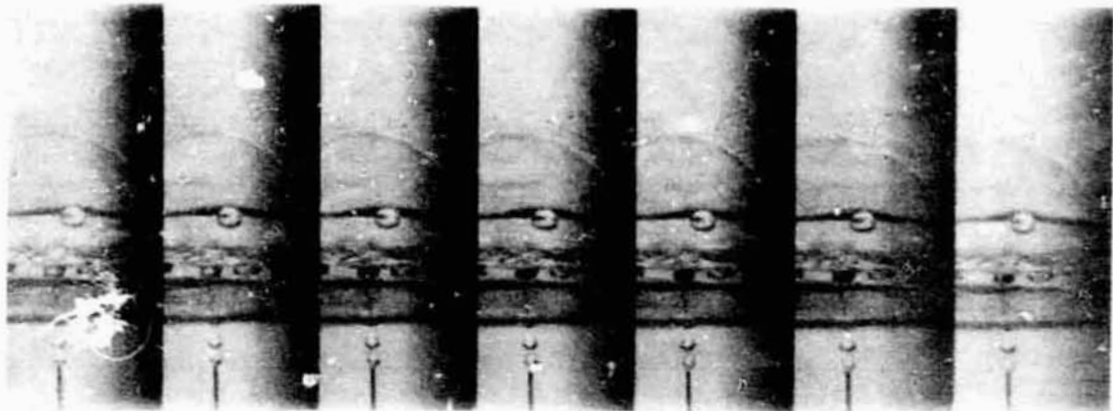
References

- Azhel, D. SL and TS LEE : "Acoustic resonance theory for the film cap of a gas bubble at a horizontal gas-liquid interface". Int. Conf. on momentum, Heat and mass transfer in two phase system. Dubrovnik, september 1970.
- Blanchard, D.C. : "The Electrification of the Atmosphere by Particles from Bubbles in the Sea". Extr. de "Progress in Oceanography", Vol.1, pp. 73 & 202, Pergamon Press, 1963.
- Blanchard, D.C. and Syzek, L.D. : "Concentration of Bacteria in Jet drops from Bursting Bubbles". Journal of Geophysical Research, Vol.77, n° 22, september 1972.
- Detwiller, A. and Blanchard, D.C. : "Aging and Bursting Bubbles in Trace-Contaminated Water". Chemical Engineering Science, Vol.33, pp. 9-13, Pergamon Press, 1978.
- Ivanov, I.B., Radoev, B., Manev, E. and Scheludko, A. : "Theory of the Critical Thickness of Rupture of Thin Liquid Film". Transactions of the Faraday Society, 66, n° 569, part.5, pp. 1262-1273, may 1970.
- Kientzler, C.F., Arons, A.B., Blanchard, D.D. and Woodcock, A.H. : "Photographic Investigation of the Projection of Droplets by Bubbles Bursting at a Water Surface". Tellus, Vol.6, n° 1, pp. 1-7, february 1954.
- McIntyre, F. : "Bubbles : A Boundary Layer "Microtome" for Micron-Thick Samples of a Liquid Surface". Journal of Physical Chemistry, Vol.72, n° 2, pp. 589-592, february 1968.
- McIntyre, F. : "Flow Patterns in Breaking Bubbles". Journal of Geophysical Research, Vol.77, n° 27, pp. 5211-5228, september 1972.
- McIntyre, F. : "Non-Lipid-Related Possibilities for Chemical Fractionation in Bubble Film Caps". J. R. O., pp. 515-527, 1974.
- Quinn, J.A., Steinbrook, R.A. and Anderson, J.L. : "Breaking Bubbles and the Water-to-Air Transport of Particulate Matter". Chemical Engineering Science, Vol.30, pp. 1177-1184, Pergamon Press, 1975.
- Scheludko, A. : "Thin Liquid Films". Advances in Colloid and Interface Science, t.1, pp. 391-464, 1967.
- Toba, Y. : "Drop Production by Bursting of Air Bubbles on the Sea Surface, 2, Theoretical Study of the Shape of floating bubbles". J. Oceanogr. Soc. Jap., 15, 1, 1959.

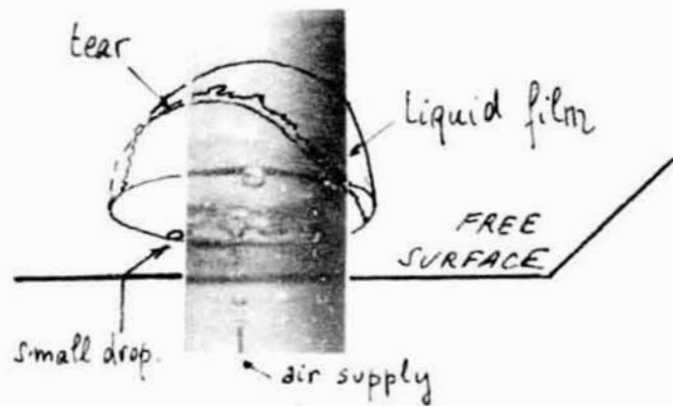


BUBBLE BURSTING AT AN AIR-LIQUID INTERFACE

ORIGINAL PAGE
BLACK AND WHITE PHOTOGRAPH



Film cap tear . 7.500 frames per second.



ORIGINAL PAGE
BLACK AND WHITE PHOTOGRAPH



JET N:1



JET N:2

Jet drops - 1.500 frames per second.